Nuclear Physics B208 (1982) 381–396

LARGE p_T QUARKONIUM PRODUCTION AT ULTRAHIGH ENERGIES

R. BAIER

Fakultät für Physik, Universität Bielefeld, D-4800 Bielefeld 1, Fed. Rep. Germany

R. RÜCKL

Sektion Physik, Universität München, D-8000 München 40, Fed. Rep. Germany

Received 1 April 1982
(Revised 5 July 1982)

We discuss large p_T charmonium, bottomonium as well as toponium production at the ultrahigh energies of the $p\bar{p}$ collider and the Isabelle pp machine. Predictions are presented for the lowest lying S- and P-wave states of each system. Our analysis is based on elements of perturbative QCD and the non-relativistic quarkonium picture. The same model successfully describes large p_T J/ψ and Y production at FNAL and ISR energies.

1. Introduction

In the next decade exciting and clarifying results can be expected from new accelerators operating at ultrahigh energies. Two representatives of the next generation of hadron-hadron machines are the proton-antiproton collider ($\sqrt{s} = 540$ GeV) at CERN which is already producing the first data and the proton-proton storage ring Isabelle ($\sqrt{s} \sim 800$ GeV) at BNL which is presently under construction. The physics program proposed for these machines covers a wide spectrum of high-energy phenomena [1]. Among these, heavy flavour production has gained much interest and consideration. Charm and bottom which are by now accepted as fundamental fermion flavours will be investigated further and, of course, one will search for new and heavier flavours such as the awaited top.

Concerning the experimental prospects of detecting new quark flavours, heavy quark–antiquark bound states have played an extraordinary role at present energies because of their striking narrowness. Theoretically, they serve as an excellent laboratory for studying the structure of hadrons and quark–gluon dynamics. Thus, it is certainly important to investigate quarkonium production at ultrahigh energies. On the theoretical side, predictions have been worked out for some general aspects, such as total rates, on the basis of experimental results at lower energies ($\sqrt{s} \lesssim 60$ GeV) and approximate scaling laws as well as in the framework of specific dynamical models. To allow for a rough orientation and to provide a measure of our predictions on details of the production pattern, we briefly rederive the order

of magnitude of the expected quarkonium cross sections. The measured excitation curves of J/ψ and Υ [2] indicate that the J/ψ cross section has essentially reached its asymptotic value in the ISR energy range, whereas the Υ cross section is still rising. This provides an absolute normalization for the J/ψ production expected at $\sqrt{s} \gg 60$ GeV, to wit

$$B_{\mu\mu} \frac{d\sigma}{dy} (J/\psi; y = 0) \sim 10^{-32} \text{ cm}^2 . \tag{1}$$

The Υ and ζ (lightest $^3S_1$ state of toponium) cross sections can, then, be estimated by employing the scaling law of ref. [3]:

$$\frac{d\sigma}{dy} (V; y = 0) \simeq \frac{\Gamma_h^V}{M_V^3} f\left(\frac{M_V}{\sqrt{s}}\right), \tag{2}$$

which follows from rather model-independent arguments. V denotes a particular resonance with mass M_V and hadronic width Γ_h^V and $f(\tau)$ is a universal function. It has been shown [2, 3] that the data on ϕ, J/ψ, ψ', Υ and Υ' are roughly consistent with this conjecture. Using the fact that $f(\tau) \sim \text{const}$ for $\tau = M_V/\sqrt{s} \leqslant 3.1/63 \sim 0.05$ and substituting measured values [4] for the resonance parameters M_Υ, Γ_h^Υ and $B_{\mu\mu}^\Upsilon$ one predicts from eqs. (1) and (2) that

$$B_{\mu\mu} \frac{d\sigma}{dy} (\Upsilon; y = 0) \sim 10^{-34} \text{ cm}^2 . \tag{3}$$

As far as toponium is concerned there is, at present, no experimental evidence for its existence. To be more specific, for a top-quark charge $e_t = \frac{2}{3}$ and for $\Gamma_{ee}^\zeta \Gamma_h^\zeta / \Gamma_{tot}^\zeta > 1$ keV, the various PETRA experiments have set a lower limit on the ζ mass [5]:

$$M_\zeta > 37 \text{ GeV} . \tag{4}$$

Choosing a mass slightly bigger, for definiteness $M_\zeta = 40$ GeV, one estimates for ζ production in hadronic collisions at $\sqrt{s} \gtrsim 800$ GeV

$$B_{\mu\mu} \frac{d\sigma}{dy} (\zeta; y = 0) \sim 10^{-36} \text{ cm}^2 , \tag{5}$$

if one takes $\Gamma_h^\zeta \sim 30$ to 50 keV and $B_{\mu\mu}^\zeta \sim 10\%$ as expected in the standard quarkonium picture [6, 7]. A number similar to eq. (5) also results from a different analysis [8] which makes use of a relation between quarkonium and massive Drell–Yan pair production.

We believe that these estimates are quite reliable. On the other hand, integrated cross sections put only weak restrictions on theoretical models, at least in this case. If one wants to discriminate between various production mechanisms it is essential to investigate more detailed structures. In the following analysis we focus on transverse momentum distributions. Clearly, predictions on such differential properties necessitate further assumptions. The existing data do not exhibit a simple

scaling behaviour but show a rather complex dependence on the flavour type, the c.m.s. energy and p_T. Thus, one needs a definite dynamical model.

In an earlier work [9] we have analyzed high p_T J/ψ and Υ production at FNAL and ISR energies in a theoretical framework which is based on perturbative QCD subprocesses between the constituents of the colliding hadrons and on the non-relativistic potential model for heavy quark–antiquark bound states. We were able to achieve a quite satisfactory and complete description of the p_T distributions* of J/ψ and Υ observed in pp collisions [2, 10]. Moreover, basically the same picture is also consistent with the observed features of inelastic J/ψ muoproduction [11]. It is this overall agreement between theory and experiment at present energies [12] which encourages us to rely on this particular model for the purpose of investigating large p_T quarkonium production at collider and Isabelle energies. The actual examination of our predictions in future experiments would provide a crucial test of the underlying theoretical picture.

An incomplete and preliminary account of our investigations was given at the 1981 Isabelle Workshop [12]. In the present paper we summarize and discuss our final results in more detail. First, we briefly introduce the model, outline our calculations and comment on the input parmeters. Then, we describe the expected pattern for the lowest-lying S- and P-wave states of the charmonium and bottomonium system. Finally, we speculate about toponium and discuss, in particular, the large p_T production of the most prominent states of the toponium spectrum assuming a typical mass of 45 GeV. All our predictions are made for $p\bar{p}$ collisions at $\sqrt{s} = 540$ GeV and/or pp collisions at $\sqrt{s} = 800$ GeV. We find, however, practically no difference between $p\bar{p}$ and pp collisions and very little variation with energy for quarkonium production in this asymptotic region as long as $x_T = 2p_T/\sqrt{s} \ll 1$.

2. The model

Here, we do not want to dwell on the subtleties of the model nor on the details of the formalism. This part can be found elsewhere [13]. However, in order to make the present discussion self-contained we would like to give a brief description of the essential elements of our approach.

2.1. BASIC ASSUMPTIONS

Concerning the origin of the hidden flavour and the formation of heavy resonances in hadronic collisions we make the following assumptions:

(i) The heavy resonances are non-relativistic quark–antiquark bound states as described by the usual potential models.

* According to I. Stumer the data in fig. 1b of ref. [2] are not plotted correctly. For the correct invariant spectra see, for example, refs. [12, 13].

(ii) At large transverse momentum the production of the heavy quark pair is dominated by QCD subprocesses of third order in the strong coupling constant α_s: $gg \to Q\bar{Q}g$, $gq \to Q\bar{Q}q$ and $q\bar{q} \to Q\bar{Q}g$. The initial quarks and gluons are the constituents of the colliding hadrons. The final light quarks and gluons materialize as jets of hadrons recoiling against the $Q\bar{Q}$ system.

(iii) The coupling of a specific bound state to the $Q\bar{Q}$ pair is directly determined by the appropriate wave function which includes all relevant quantum number projections in conformity with the spin (s), angular momentum (L), charge conjugation and the colour singlet nature of the bound state considered.
We use two notations to refer to a particular bound state, either the usual quantum number characterization, $^{2s+1}L_J$, or the symbols defined in table 1.

The direct formation of heavy resonances at short distances, which is the essence of assumption (iii), has a number of important consequences. It leads to spin and colour selection rules which affect the relative weight of the contributions from the various subprocesses (ii) to a given resonance decisively. This is illustrated in fig. 1. For example, $^3S_1$ states can only be produced via $gg \to {}^3S_1 g$ whereas $^1S_0$ and ^3P_J states receive contributions from all $O(\alpha_s^3)$ subprocesses. Of course, $^3S_1$ resonances also originate from decays of heavier states of the same system. This possibility, however, can be disregarded in most cases. The only important contributions come from P-wave production and subsequent decay, $^3P_J \to {}^3S_1\gamma$. Furthermore, assumption (iii) distinguishes the model considered here from another approach [14] which proceeds from the same mechanisms (ii) for heavy flavour production but assumes that the bound states are formed afterwards by soft processes. This formation is, therefore, not calculable perturbatively in contrast to what we suggest. Instead, one assumes that the bound-state formation does not affect the kinematics of processes (ii), and that the absolute yields can be estimated in an average sense by employing semilocal duality [13, 14]. As far as predictions of this model for large p_T and ultrahigh energies are concerned, we only known of the result on Υ production in $p\bar{p}$ collisions at $\sqrt{s} = 540$ GeV reported in ref. [14].

Presently, it cannot be decided from first principles which of these two pictures describes the bound-state formation correctly because of our failure to understand the long-range QCD interactions quantitatively. For instance, it could well be that soft gluons play an important dynamical role in the production processes considered in this paper. If so they would very likely vitiate any meaning of colour counting (apart from possible effects on the normalizations). In this case, the colour selection rules mentioned above should be dropped. On the other hand, colour counting makes sense (in fact originated) even in light quark systems as illustrated impressively by the puzzling success of hadron spectroscopy in the nonrelativistic quark model. There, gluons are supposed to build up the constituent quarks but are otherwise not considered as dynamical degrees of freedom. In the same spirit we disregard soft gluons by coupling the $Q\bar{Q}$ pair directly to a particular quarkonium state. This, then, enables us to make definite and quantitative predictions some of which

TABLE 1

Charmonium ($c\bar{c}$), bottomonium ($b\bar{b}$) and toponium ($t\bar{t}$) parameters used in our calculations

Parameters		$c\bar{c}$		$b\bar{b}$		$t\bar{t}$	
Masses (GeV)	$^1S_0$	η_c	2.983	η_b	9.0	η_t	45.0
		η_c'	3.592	η_b'	10.0	η_t'	45.6
	$^3S_1$	J/ψ	3.097	Υ	9.46	ζ	45.0
		ψ'	3.685	Υ'	10.02	ζ'	45.6
				Υ''	10.30	ζ''	45.9
						ζ'''	46.0
	^3P_J	χ_{0c}	3.414	χ_{0b}	9.9	χ_{0t}	45.5
		χ_{1c}	3.507	χ_{1b}		χ_{1t}	
		χ_{2c}	3.551	χ_{2b}		χ_{2t}	
Leptonic widths (keV)		J/ψ	4.8	Υ	1.2	ζ	4.8
		ψ'	2.0	Υ'	0.6	ξ'	1.8
				Υ''	0.4	ζ''	1.0
						ζ'''	0.9
	r [eq. (9)]		0.074		0.013		0.001
	$\alpha_s(M^2)$		0.4		0.26		0.19
Branching ratios %	$^3S_1 \to \mu^+\mu^-$	J/ψ	7.4	Υ	3.5	ζ	10
	$^3P_J \to {}^3S_1\gamma$	χ_{0c}	2.7	χ_{0b}	4	χ_{0t}	100
		χ_{1c}	31.5	χ_{1b}	29	χ_{1t}	
		χ_{2c}	15.4	χ_{2b}	10	χ_{2t}	

Detailed references are given in the text.

directly reflect the presence of colour, spin, etc. selection rules. It should therefore, be possible to decide phenomenologically whether our conjecture is correct.

2.2. CALCULATION AND INPUT PARAMETERS

Typical QCD diagrams contributing in lowest order to the subprocesses $gg \to ({}^1S_0, {}^3S_1, {}^3P_J)g$, $gq \to ({}^1S_0, {}^3P_J)q$ and $q\bar{q} \to ({}^1S_0, {}^3P_J)g$ are shown in fig. 1. Those which have to be added in order to obtain a gauge-invariant set in $O(\alpha_s^3)$ are easily constructed by permuting the gluon lines. For brevity, we do not give explicit formulas for the corresponding cross sections (see ref. [13]). Their schematical structure in the non-relativistic limit is as follows:

$$\frac{d\hat{\sigma}}{d\hat{t}}(ab \to {}^{2s+1}L_J c) = \frac{\alpha_s^3}{\hat{s}^2} f(ab \to {}^{2s+1}L_J c; \hat{s}, \hat{t}, \hat{u}, M^2) \times \begin{cases} |R_S(0)|^2/M^3, & \text{for S-waves}, \\ |R_P'(0)|^2/M^5, & \text{for P-waves}. \end{cases} \tag{6}$$

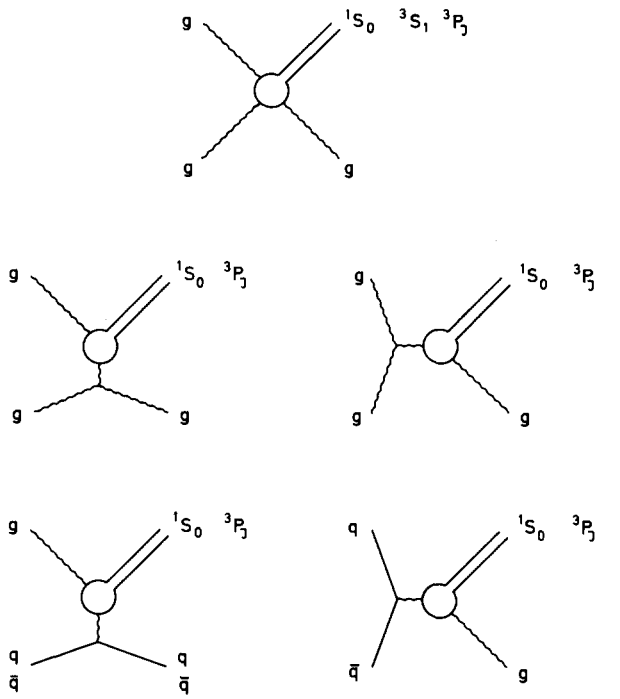

Fig. 1. Typical diagrams contributing to $O(\alpha_s^3)$ hadroproduction of heavy quarkonia at large transverse momentum.

Here, $R_S(0)$ and $R'_p(0)$ denote the non-relativistic S-wave function and the derivative of the P-wave function, respectively, at the origin. The dynamics is characterized by the function f of the usual Mandelstam variables $\hat{s}$, $\hat{t}$ and $\hat{u}$. Since for a non-relativistic system the binding energy is small with respect to the constituent mass we always make use of the approximation

$$M \simeq 2m_Q\,, \tag{7}$$

where M and m_Q are the resonance and quark mass, respectively.

The numerical values of the various resonance parameters used throughout this paper are listed in table 1. For the charmonium and bottomonium wave functions, $|R_S(0)|^2$, we take the values which follow from the measured leptonic widths $\Gamma_{ee} \equiv \Gamma(^3S_1 \to e^+e^-)$ and the familiar lowest order relation

$$|R_S(0)|^2 = \frac{M^2\Gamma_{ee}}{4\alpha^2 e_Q^2}\,. \tag{8}$$

For the toponium system we adopt the results of a specific* quarkonium model

* Model II in refs. [15, 16].

calculation by Krasemann and Ono [15] and Krammer and Krasemann [16]. This model predicts almost constant values of Γ_{ee}/e_Q^2 from the charm-quark mass up to a top-quark mass $m_t \sim 20$ GeV. A similar result is obtained in a recent analysis by Buchmüller and Tye [7]. As far as the P-wave functions are concerned, the authors of ref. [16] find $|R'_P(0)|^2/m_Q^3 \simeq 0.024\ \text{GeV}^2$ for charm, $0.012\ \text{GeV}^2$ for bottom, and $0.007\ \text{GeV}^2$ for top. One sees that this particular ratio varies relatively slowly with the quark mass. For convenience, we work instead with the dimensionless parameter

$$r = \frac{4|R'_P(0)|^2}{M^2|R_S(0)|^2} \tag{9}$$

calculated from the quoted ratios and eq. (8). The numerical values can be found in table 1. It is interesting to note that with $r = 0.074$ for charmonium and $\alpha_s(M_\psi^2) \simeq 0.4$ one predicts [17] $\Gamma_h(\chi_0) \sim 11$ MeV in remarkable agreement with the measured total width $\Gamma_{tot}(\chi_0) = 10 \pm 3$ MeV [4]. Since the radiative width $\Gamma(\chi_0 \to J/\psi\gamma) \sim 100$ keV is very small, $\Gamma_{tot} \sim \Gamma_h$. One should keep in mind, however, that such agreements could be accidental because of relativistic and higher order QCD corrections. The former, at least, cannot be taken into account appropriately without knowing more about QCD bound states. On the other hand, these corrections should become less important as the quark mass becomes heavier.

One particular aspect of higher order corrections is their implication on the correct choice of the effective QCD scale Λ in the one-loop running coupling constant (f = number of active flavours):

$$\alpha_s(Q^2) = 12\pi/(33 - 2f) \ln \frac{Q^2}{\Lambda^2}. \tag{10}$$

In our lowest order calculations we take $\Lambda = 500$ MeV which is not necessarily inconsistent with the smaller value $\Lambda \sim 100$ MeV suggested by the hadronic widths of the J/ψ and Υ since the higher order corrections are, in general, different for a production and a decay process. Unfortunately, we cannot prove that for the moment since we do not know the higher order corrections to our subprocesses. All we can say is that phenomenologically within our framework one needs such a big Λ in order to explain, for example, the magnitude of the J/ψ yields at large transverse momentum at $\sqrt{s} = 63$ GeV [9]. It could be that this necessity is a consequence of neglecting higher twist contributions to the production cross sections. At present, it is simply not known how to incorporate such effects properly. Qualitatively, however, one expects higher twist processes to die out relatively to the lowest order QCD mechanisms as p_T increases due to their different scaling behaviour. At any rate, our predictions for the heavier resonances Υ, ζ, etc. are much less sensitive to the value of Λ one actually chooses. A further but minor ambiguity is connected with the scale Q^2 which is also supposed to control scaling violations. We think that $Q^2 = M^2 + p_T^2$ is a reasonable choice.

Having at hand the cross sections for the various subprocesses of fig. 1 one obtains the inclusive cross sections $E(\mathrm{d}^3\sigma/\mathrm{d}^3p)$ (p or $\bar{\mathrm{p}}+\mathrm{p}\to {}^{2s+1}L_J+\mathrm{X}$) by convolution of the former with the appropriate quark and gluon structure functions according to the usual hard scattering formalism. For the parton densities we use the same parametrizations as in our previous analysis [9, 11] of hadro- and leptoproduction of J/ψ and Υ. One set is a simple scaling parametrization [18], the other one [19] includes scale-violating effects in accordance with the leading log QCD evolution equations. It turns out that the first set is slightly preferred by the ISR data. Quite generally, one finds that the data favour a relatively hard gluon distribution of the effective form $xG(x)=3(1-x)^5$.

3. Production of charmonium and bottomonium states

Our numerical results are presented in two separate sections. First, we focus on the charmonium and bottominum system. In their case, one knows how well the potential model works. Furthermore, we have shown that the particular model for quarkonium production outlined in the last section successfully describes the large p_T data on J/ψ and Υ in the FNAL/ISR energy range. Then, we discuss toponium production which is much more speculative, at least as far as the spectroscopy part is concerned.

3.1. INVARIANT CROSS SECTIONS FOR $^1S_0$, $^3S_1$ and ^3P_J STATES

Fig. 2 summarizes our predictions on the invariant cross sections $E\,\mathrm{d}^3\sigma/\mathrm{d}^3p$ at $\theta_{\mathrm{cm}}=90°$ for the lowest lying S- and P-wave resonances of the (a) charmonium and (b) bottomonium system. Curves are only drawn for $\mathrm{p\bar{p}}$ collisions at $\sqrt{s}=540$ GeV. For pp collisions and similar energies one finds essentially the same result, as pointed out in the introduction. Furthermore, the $^3S_1$ yields plotted in fig. 2 are those which are produced exclusively by the direct process $\mathrm{gg}\to {}^3S_1\mathrm{g}$. Contributions from radiative ^3P_J decays will be included later. One notices a striking hierarchy in the production cross sections: $^1S_0 > {}^3P_J > {}^3S_1$. The details are due to a rather complicated interplay of various effects involving wave functions, thresholds and differences in the dynamics of the subprocesses. Also the difference between the gluon and quark structure functions is important for the obtained pattern.

In the following we comment on the most conspicuous structures apparent in fig. 2: (i) The relative yields $1^1S_0 : 2^1S_0$ as well as $n^3S_1 : m^3S_1$ essentially reflect the ratios of the corresponding wave functions, $|R_{n\mathrm{S}}(0)|^2$, or leptonic widths, $\Gamma(n\mathrm{S}\to \mathrm{e^+e^-})$, apart from a weak dependence on mass, transverse momentum and spin. (ii) At $p_T^2 \gg M^2$, the P-waves are produced in fixed proportions, $^3P_0 : {}^3P_1 : {}^3P_2 = 1:6:2$, which are determined by the cross sections of the corresponding subprocesses [13]. (iii) The relative abundance of $^1S_0$ to ^3P_J is controlled by the parameter r of eq. (9). More precisely, at sufficiently large p_T one finds [13] $^1S_0 : {}^3P_0 \sim 1/r$

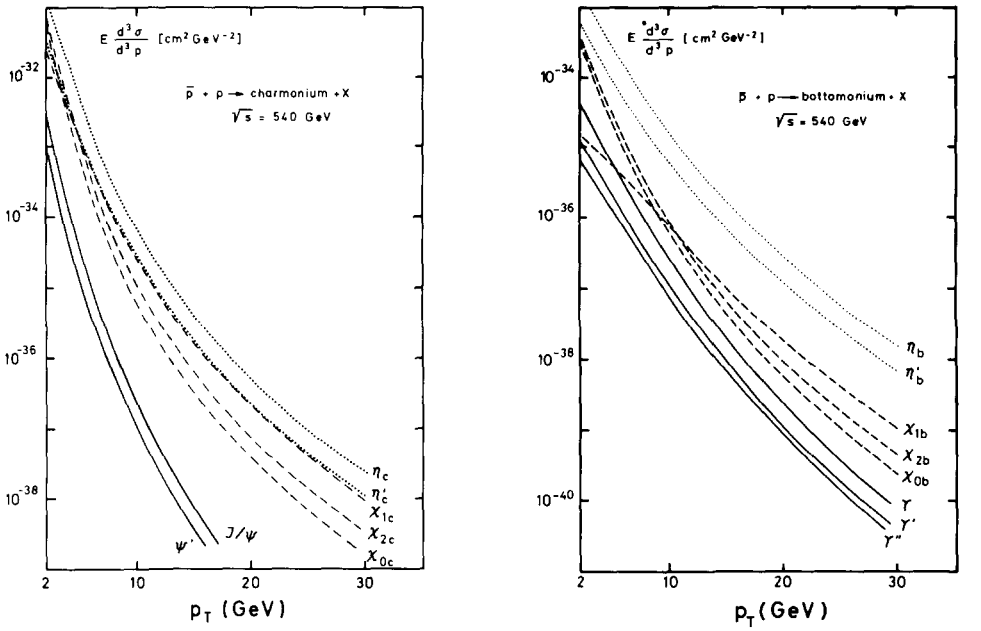

Fig. 2. Invariant cross sections at $\theta_{cm} = 90°$ versus p_T for some of the lightest S- and P-wave states of (a) the charmonium system, (b) the bottomonium system, calculated with scaling structure functions [18] and fixed $\alpha_s(M^2)$.

whereas $^1S_0 : {}^3P_0 \sim 1/9r$ for $p_T \to 0$. The numerical coefficients of the $1/r$ behaviour follow again from the cross sections of eq. (6). (iv) Another general feature is also a consequence of the specific dynamics of S- and P-wave production at the level of the QCD subprocesses (fig. 1) in our model. One can show [9, 13] that $d\hat{\sigma}(^1S_0, {}^3P_J)/d\hat{\sigma}(^3S_1) \sim p_T^2/M^2$ at $p_T^2 \gg M^2$ which leads to different slopes in p_T for the $^1S_0$ and ^3P_J distributions, on the one side, and the $^3S_1$ distributions, on the other side. This asymptotic behaviour is clearly exhibited in the charmonium spectra of fig. 2a whereas it is not yet realized in the bottomonium spectra of fig. 2b because of the larger mass scale. It would, however, become visible at higher p_T. (v) We should finally mention that the $^3S_1$ and $^3P_1$ cross sections are finite for vanishing p_T in contrast to the $^1S_0$ and $^3P_{0,2}$ cross sections which, formally, diverge for $p_T \to 0$. We always stay away from this potentially dangerous limit.

3.2. INCLUSIVE J/ψ AND Υ SPECTRA

To obtain the fully inclusive J/ψ and Υ yields one has to consider two different sources. One is the direct production via $gg \to {}^3S_1 g$, the other one is ^3P_J production (via all of the subprocesses illustrated in fig. 1) and subsequent radiative decay, $^3P_J \to {}^3S_1 \gamma$. Other contributions of the second kind can be neglected because of low

production cross sections of the parents or small branching ratios into the lowest $^3S_1$ states or because of both. We calculate the J/ψ and Υ distributions generated by the χ_c and χ_b spectra of fig. 2 under the assumption that the latter decay isotropically with branching ratios as given in table 1. Adding, then, the direct contributions labelled by J/ψ and Υ in fig. 2, respectively, one finds the inclusive p_T distributions plotted in fig. 3 for the two representative energies $\sqrt{s} = 540$ and 800 GeV. Also shown are the theoretical J/ψ and Υ spectra [9, 12] at the highest ISR energy together with data [2]. The yields obviously continue to increase significantly at fixed p_T when one goes beyond the ISR energy. For illustration,

$$\left.\frac{E(d^3\sigma/d^3p)(\sqrt{s}=800\ \text{GeV})}{E(d^3\sigma/d^3p)(\sqrt{s}=63\ \text{GeV})}\right|_{y=0} \sim \begin{cases} 100 & \text{for } J/\psi \\ 20 & \text{for } \Upsilon \end{cases}, \tag{11}$$

at $p_T \sim 6$ GeV/c. The experimental implications are obvious.

As far as the contributions from χ production are concerned we find at ultrahigh energies that the latter dominate completely the inclusive J/ψ cross sections. In contrast, the χ_b contribution to the inclusive Υ yield is approximately of the same size as the direct contribution. However, also in the Υ case, P-wave production becomes the dominant source as p_T increases beyond the range studied in fig. 3. This pattern is quite different at ISR energies [13] where the P-wave component in the Υ cross section does not exceed the 30% level for $2 < p_T < 8$ GeV/c, while

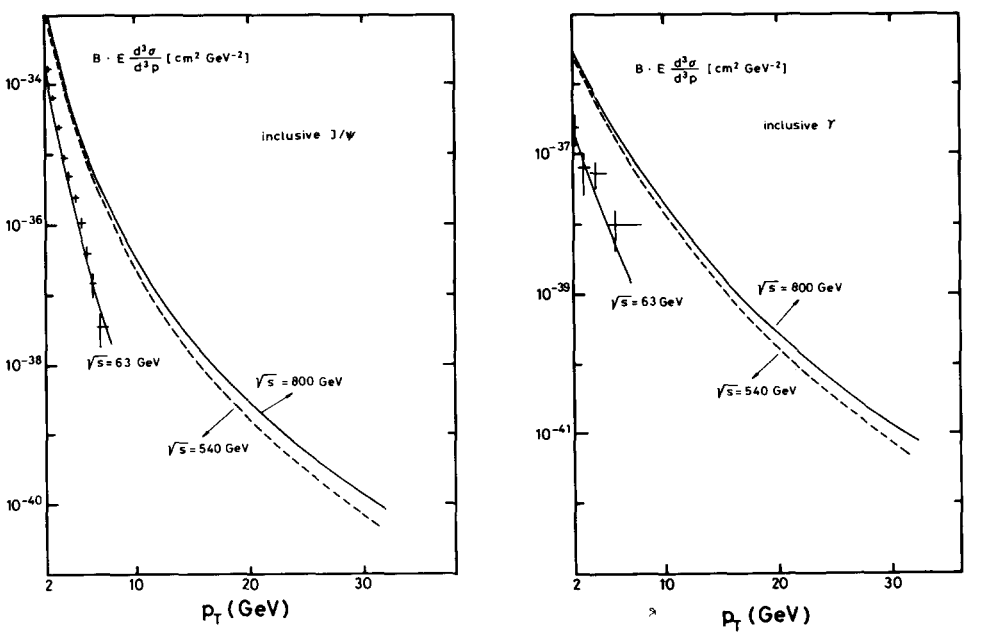

Fig. 3. Inclusive p_T distributions at $\theta_{cm} = 90°$ for (a) J/ψ and (b) Υ resulting from the spectra of fig. 2 as described in the text. Compared are the cross sections for three prominent machines: ISR, $p\bar{p}$ collider and Isabelle. The data are taken from ref. [2].

it reaches about 50% of the J/ψ cross section at $p_T \sim 2$ GeV/c and dominates the latter at $p_T \sim 7$ GeV/c. At this point we should remark that although there is a tendency of large χ production in our model, the precise magnitude depends directly on the parameter r and is, therefore, disputable to the same extent as the P-wave functions of the quarkonium model.

4. Production of toponium states

We now turn to large p_T toponium production at collider and Isabelle energies. For the 1^- ground-state mass of toponium we choose 45 GeV which is just above the present lower limit [5]. The remaining toponium parameters used in our numerical calculations are discussed in sect. 2 and listed in table 1. Fig. 4 shows the resulting invariant cross sections for the lightest S- and P-wave states at $\sqrt{s} = 540$ GeV. As expected, the general pattern is not very different from the one found in the case of charmonium and bottomonium production. The similarity becomes particularly apparent if one compares fig. 4 with the bottomonium distributions at $p_T \lesssim M_\Upsilon \sim 10$ GeV (fig. 2b). Thus, the explanation of the main features given in subsect. 3.1 applies here as well. For example, the further decrease of P-wave production relative to S-wave production which can be clearly seen by comparing figs. 4 and 2b simply reflects the corresponding decrease of the parameter r defined in eq. (9), numerically $r(b\bar{b})/r(t\bar{t}) \sim 10^{-1}$. From fig. 4 one also concludes that P-wave contributions to the inclusive ζ yields are completely negligible for $p_T > 15$ GeV/c. For smaller transverse momenta, however, a sizable fraction of ζ's

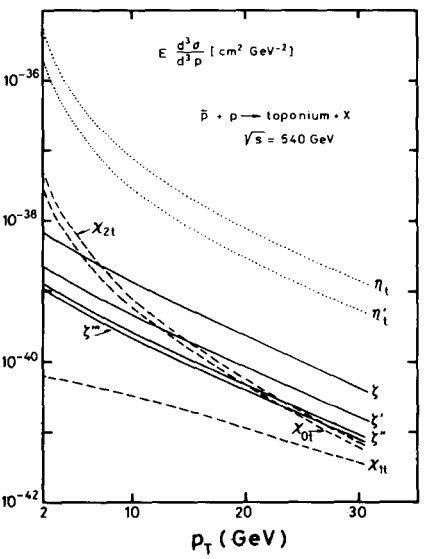

Fig. 4. Invariant cross sections at $\theta_{cm} = 90°$ versus p_T for some of the lightest S- and P-wave states of toponium with $M_\zeta = 45$ GeV calculated in the scaling limit similarly to fig. 2.

could still come from χ_{0t} and χ_{2t} decays if the branching ratios into the ζ are large. This is indeed the case. Combining results of refs. [15–17] we derive branching ratios for $\chi_t \to \zeta\gamma$ which are typically larger than 50%. This is not too surprising since the dipole moments $\langle {}^3P_J|r|{}^3S_1\rangle$ decrease relatively slowly with increasing quark mass. For the purpose of estimating the contributions from χ_t production to the inclusive ζ yields we simply take $B(\chi_t \to \zeta\gamma) \sim 100\%$ which is sufficiently accurate considering the overall uncertainties in the toponium parameters. At any rate, it gives an upper limit. Assuming again that the χ_t states decay isotropically and adding the contributions from the direct process $gg \to \zeta g$ (curve labelled by ζ in fig. 4) one obtains the inclusive ζ distribution plotted in fig. 5. Note that the leptonic branching ratio $B^{\zeta}_{\mu\mu} \sim 10\%$ [6] is included in the normalization.

Fig. 5 also summarizes our predictions on J/ψ and Υ production. The full curves represent the results obtained with scaling structure functions [18] and fixed $\alpha_s(M^2)$ (see table 1) similarly to the results shown in figs. 2 to 4. The dashed curves are calculated with the running coupling constant $\alpha_s(M^2+p_T^2)$ given in eq. (10) and with the structure functions of ref. [19] which include scale-violating effects. Whereas QCD evolution leads to a faster fall off of the J/ψ and Υ yields with p_T it only affects the normalization of the ζ distribution without changing the slope appreciably. This is because $p_T^2 \ll M_\zeta^2$ for most of the transverwe momenta studied in fig. 5 such that the scale $Q^2 = M^2 + p_T^2$ does not run very much in the ζ case.

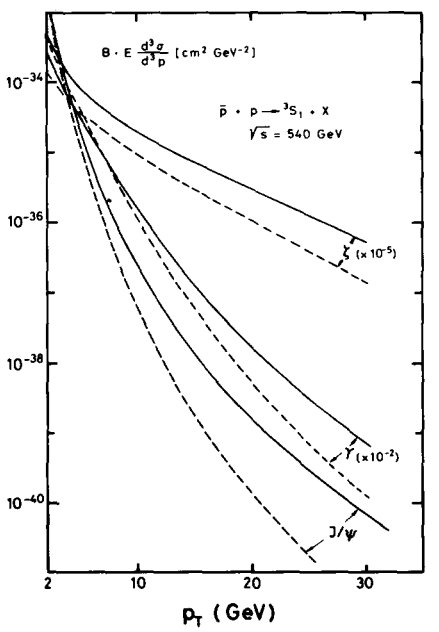

Fig. 5. Comparison of the inclusive p_T distributions of J/ψ (3.1), Υ(9.5) and ζ(45) at $\theta_{cm} = 90°$. The full curves are scaling predictions, the dashed curves include scale-violating effects. The leptonic branching ratios B are as given in table 1.

The arrows in fig. 5 indicate the range of variation which must be considered as uncertain. At this point we should remind the reader that the gluon density plays a particularly important role as can be seen from the subprocesses of fig. 1. It is unfortunate that exactly this structure function is not too well known, at least for large x and large Q^2. Nevertheless, fig. 5 can serve as a useful estimate of what one can expect at ultrahigh energies. We believe that, in particular, the relative yields are reliable provided that the quarkonium parameters of table 1 are correct. An interesting and firm prediction is also the flattening of the p_T distributions as the resonances become heavier. This behaviour can effectively be described by $E\,\mathrm{d}^3\sigma/\mathrm{d}^3p \sim (M^2+p_T^2)^{-n(p_T)}$ where $n(p_T)\sim 3$ for $2<p_T<10$ GeV/c.

We have also considered the possibility that the 1^- toponium ground state has a larger mass than ~45 GeV as assumed in the analysis discussed so far. Since the predicted toponium yields are already rather small for the most optimistic mass assignment possible, we do not present details for higher values of M_ζ. For completeness, we mention, however, that at intermediate p_T the inclusive ζ yields fall with increasing M_ζ roughly as follows:

$$E\frac{\mathrm{d}^3\sigma}{\mathrm{d}^3p}\bigg|_{y=0}(M_\zeta = 40, 60, 80, 100\ \mathrm{GeV}) \sim 1 : 10^{-1} : 2\cdot 10^{-2} : 10^{-2}\,. \qquad (12)$$

Apart from minor variations* due to the leptonic widths which increase slightly [15, 16], the above proportions follow simply from the effective distribution $E(\mathrm{d}^3\sigma/\mathrm{d}^3p)\sim(M^2+p_T^2)^{-3}$ mentioned above.

Finally, one should keep in mind that all our estimates on ζ are obtained under the assumption that the ratio Γ_{ee}/e_Q^2 has the same value for the ζ as for the J/ψ and Υ. This result, of course, depends crucially on how one extrapolates the potential from distances characteristic for J/ψ and Υ down to the smaller distance scale of the ζ. For a pure Coulomb potential, for example, one has [20] $\Gamma_{ee}\sim M$ in contrast to a linear potential which gives $\Gamma_{ee}\sim 1/M$. It is not excluded that at the toponium the binding is already dominated by the one-gluon exchange and, therefore, Coulomb-like. In this case, $\Gamma_{ee}^{\zeta} \gg \Gamma_{ee}^{\psi}$ such that the actual production rates of ζ at large p_T could considerably exceed the predictions presented in fig. 5.

As a reminder, although we specified our results for $p\bar{p}$ collisions at $\sqrt{s}=$ 540 GeV, numerically they also apply within the uncertainties to pp collisions at $\sqrt{s}=800$ GeV.

5. Summary

We have presented predictions on large p_T charmonium, bottomonium and toponium production at the ultrahigh energies of the $p\bar{p}$ collider and the Isabelle

* We have disregarded possible neutral current effects if $M_\zeta \sim M_{Z^0}$. These are not expected to change significantly the high p_T features discussed here.

machine. In particular, we have discussed in detail the expected p_T distributions at $\theta_{cm} = 90°$, individually for the first few $^1S_0$, $^3S_1$ and ^3P_J states of each system and inclusively for $J/\psi(3.1)$, $\Upsilon(9.5)$ and $\zeta(45)$. Our analysis is based on perturbative QCD subprocesses in which the heavy quark–antiquark bound states are represented by their non-relativistic wave functions. For the various quarkonium parameters which enter our numerical calculations we take either experimental numbers or theoretical values obtained in a potential model. The structure functions of the nucleon are those commonly used for other hard scattering processes.

Our main results can be summarized as follows:

(i) The production cross sections follow a remarkable and quite general pattern: $^1S_0 > {}^3P_J > {}^3S_1$. As the quark mass increases the P-wave production decreases relative to the S-wave production. Particularly striking are the large $^1S_0$ cross sections. It is interesting to contemplate the possibility to detect such states (e.g. η_c and η_b) in hadronic reactions. This will not be easy. On the other hand, these states are also hard to see in e^+e^- annihilation. In any case, such an experiment does not seem unfeasible since one can afford to search in a channel which gives a good signal even if it has a rather small branching ratio.

(ii) The inclusive J/ψ yield is dominated by χ_c production and radiative decay $\chi_c \to J/\psi\gamma$ at all $p_T > 2$ GeV/c. In contrast, the inclusive Υ yields at $p_T < 30$ GeV/c as well as the inclusive ζ yields at $p_T < 15$ GeV/c receive roughly equal contributions from both sources, from P-waves and from the direct process $gg \to {}^3S_1 g$. At $p_T^2 \gg M^2$, the P-wave contribution becomes more and more important since $d\sigma({}^3P_J)/d\sigma({}^3S_1) \sim p_T^2/M^2$.

(iii) At fixed $\sqrt{s}$ and $\theta_{cm} = 90°$ the invariant cross sections behave effectively like $(M_T^2 + p_T^2)^{-n(p_T)}$ as long as $x_T = 2p_T/\sqrt{s} \ll 1$. Consequently, the slope in p_T is the flatter the heavier the resonance.

(iv) The magnitude of the expected cross sections suggests that it should not be too hard to observe the large p_T production of J/ψ and Υ at Isabelle ($\mathcal{L} = 10^{32}\,\mathrm{cm}^{-2}\,\mathrm{sec}^{-1}$), at least up to transverse momenta of 10 to 15 GeV/c. At this value of p_T the cross sections are predicted to be of the order of the J/ψ and Υ cross sections measured at the highest ISR energy and $p_T \sim 6$ GeV/c. For the toponium ground state, $\zeta(45)$, we find at $\theta_{cm} = 90°$ and $p_T \sim 2$ GeV/c, $B_{\mu\mu} E\, d^3\sigma/d^3p \sim 10^{-39}\,\mathrm{cm}^3\,\mathrm{GeV}^{-2}$ which is probably too small to obtain reasonable statistics. There could, however, be a change if the quarkonium potential is more Coulomb-like than assumed in our analysis. As pointed out this would lead to a considerably larger value of $|R_S(0)|^2$ or, equivalently, Γ_{ee}. In any case, because of the much smaller luminosity expected for the $p\bar{p}$ collider, $\mathcal{L} \sim 10^{29}\,\mathrm{cm}^{-2}\,\mathrm{sec}^{-1}$, it seems rather hopeless to study the large p_T production of any of the considered resonances at such a machine.

(v) Concerning the experimental feasibility to detect toponium bound states one must also worry about the possible background besides the low production rates. The most competing source of high p_T dimuons are the familiar QCD processes

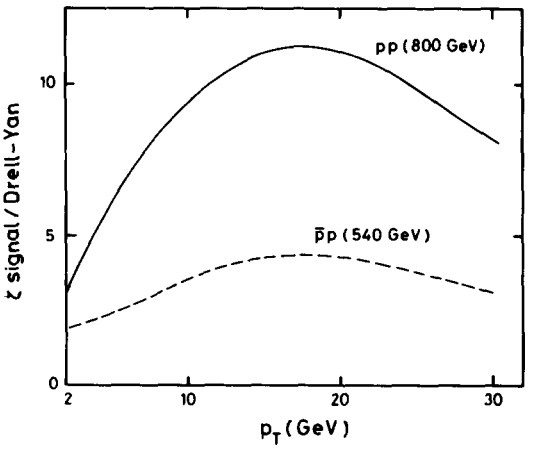

Fig. 6. Signal to background ratio for high p_T dimuons originating from ζ and Drell–Yan pair production for the $p\bar{p}$ collider and Isabelle.

$qg \to q\gamma(\to \mu^+\mu^-)$ and $q\bar{q} \to g\gamma(\to \mu^+\mu^-)$ [21]. We have estimated the signal to background ratio for $\zeta(45)$ assuming a mass resolution of 1 GeV. For consistency with our lowest order quarkonium calculation, we also neglect higher order QCD corrections [22] to the high p_T Drell–Yan production via the above subprocesses. Fig. 6 shows the results for pp ($\sqrt{s} = 800$ GeV) and $p\bar{p}$ ($\sqrt{s} = 540$ GeV). As can be seen, the signal to background ratio makes it again more favourable to search for heavy resonances in pp collisions at ultrahigh energies as opposed to $p\bar{p}$ collisions at similar energies.

To conclude, a confrontation of our predictions with experimental data in future experiments would serve as a decisive test of the detailed theoretical picture of quarkonium production described in this paper. The uncertainties inherent in the model, of course, complicate such a comparison. However, if one considers simultaneously the whole spectrum of predictions discussed in this paper one should still be able to sort out the dominant production mechanism.

We thank J. Cleymans and M. Kuroda for allowing us to use their program in the calculation of the Drell–Yan background. One of us (R.R.) is also grateful to W. Buchmüller for numerous discussions on quarkonium models and to the participants of the study group on New Flavours at the 1981 Isabelle Summer Workshop for interesting discussions which stimulated our detailed investigation of toponium production. The other author (R.B.) would like to thank C.W. Fabjan for a useful discussion.

References

[1] Proc. 1981 Isabelle Summer Workshop, Brookhaven National Laboratory, Upton, Long Island, New York, 11973

[2] C. Kourkoumelis et al., Phys. Lett. 91B (1980) 481;
I. Stumer, private communication
[3] T.K. Gaisser, F. Halzen and E.A. Paschos, Phys. Rev. D15 (1977) 2572
[4] Review of Particle Properties, Rev. Mod. Phys. 52 (1980) no. 2;
D.L. Scharre, Talk at Int. Conf. on Physics in collision: high energy ee/ep/pp interactions, Blacksburg, Virginia, May 28-31, 1981, SLAC-PUB-2761 (June, 1981)
[5] B. Wiik, Proc. 20th Int. Conf. on High-energy physics, Madison, 1980, AIP Conf. Proc. 68 (1981) 1379
[6] S. Pakvasa, M. Dechantsreiter, F. Halzen and D.M. Scott, Phys. Rev. D20 (1979) 2862
[7] W. Buchmüller and S.-H.H. Tye, Phys. Rev. D24 (1981) 132
[8] M. Dechantsreiter, F. Halzen, P. McIntyre and D.M. Scott, Madison preprint, DOE-ER/00881-202 (April, 1981)
[9] R. Rückl, Proc. Moriond Workshop on Lepton pair production, Les Arcs, 1981, ed. J. Tran Thanh Van (Editions Frontières, France) p. 323;
R. Baier and R. Rückl, Phys. Lett. 192B (1981) 364
[10] A.G. Clark et al., Nucl. Phys. B142 (1978) 29;
K. Ueno et al., Phys. Rev. Lett. 42 (1979) 486
[11] E.L. Berger and D. Jones, Phys. Rev. D23 (1981) 1521;
W.Y. Keung, Talk at Z_0 physics Workshop, Cornell University (1981):
R. Baier and R. Rückl, Nucl. Phys. B 201 (1982) 1
[12] R. Baier and R. Rückl, Proc. 1981 Isabelle Summer Workshop, Brookhaven National Laboratory, Upton, Long Island, New York, 11973, vol. 2, p. 542;
R. Rückl and R. Baier, Proc. Moriond Workshop on New flavours, Les Arcs, Savoie, France, 1982, ed. J. Tran Thanh Van and L. Montanet (Editions Frontières, France) p. 79
[13] R. Baier and R. Rückl, Bielefeld preprint, in preparation
[14] Z. Kunszt, E. Pietarinen and E. Reya, Phys. Rev. D21 (1980) 733
[15] H. Krasemann and S. Ono, Nucl. Phys. B154 (1979) 283
[16] M. Krammer and H. Krasemann, Acta Phys. Austr. XXI (1979) 259
[17] H. Krasemann, Z. Phys. C1 (1979) 189
[18] G. Altarelli, R.K. Ellis and G. Martinelli, Nucl. Phys. B157 (1979) 461
[19] R. Baier, J. Engels and B. Petersson, Z. Phys. C2 (1979) 265; C6 (1980) 309
[20] C. Quigg and J. Rosner, Phys. Reports 56 (1979) 167
[21] F. Halzen and D.M. Scott, Phys. Rev. Lett. 40 (1978) 1117
[22] R.K. Ellis, G. Martinelli and R. Petronzio, CERN preprint, CERN-TH/3079 (1981), Nucl. Phys. B, imprint